

# The effect of starvation on the dynamics of consumer populations

Yeakel, Kempes, & Redner

July 18, 2016

- 1        The behavioral ecology of most, if not all, organisms is influenced by the energetic state
- 2        of individuals. An individual's energetic state directly influences how it invests its stores in
- 3        an uncertain environment. Such behaviors are generally manifested as trade-offs, which often
- 4        concern investing in individual maintenance and growth (somatic effort) or allocating energy
- 5        towards reproduction (reproductive effort) (Martin, 1987; Kirk, 1997; Kempes et al., 2012).
- 6        The timing of these behaviors is often important and is under strong selective pressure, as
- 7        they tend to have large effects on the future fitness of the organism (Mangel and Clark, 1988).
- 8        To what extent, and when, organisms invest in somatic vs. reproductive expenditures may be
- 9        driven by habitat, seasonality, evolutionary history, inter- or intra-specific interactions, the
- 10      distribution of resources. Importantly, the influence of resource limitation on an organism's
- 11      ability to maintain its nutritional stores may lead to repeated delays or shifts in reproduction
- 12      over the course of an organism's life.
- 13      Maximizing fitness between growth and maintenance activities vs. reproductive efforts
- 14      in large part structures the life-history of species, and this can be achieved by alternative

15 behavioral strategies or via physiological switches, both of which are sensitive to resource  
16 availability. Behavioral changes in somatic or reproductive investment occur in response to  
17 limited resources (Morris, 1987). For example, reindeer invest less in calves born after harsh  
18 winters (when the mother's energetic state is poor) than in calves born after moderate winters  
19 (Tveraa et al., 2003), whereas many bird species invest differently in broods during periods  
20 of resource scarcity (Daan et al., 1988; Jacot et al., 2009), sometimes delaying or foregoing  
21 reproduction for a breeding season (Martin, 1987; Barboza and Jorde, 2002). Such breeding  
22 behaviors is generally referred to as *capital breeding*. Freshwater and marine zooplankton  
23 have been observed to avoid reproduction under nutritional stress (Threlkeld, 1976), with  
24 those that do reproduce evincing lower survival rates (Kirk, 1997), while artificially induced  
25 stress has been observed to decrease reproductive success in Atlantic cod (Morgan et al.,  
26 1999). Organisms may also separate maintenance and growth from reproduction over space  
27 and time. Many salmonids, birds, and some mammals return to migratory breeding sites  
28 to reproduce after one or multiple seasons in alternative environments spent accumulating  
29 body mass and nutritional reserves (Weber et al., 1998; Mduma et al., 1999; Moore et al.,  
30 2014).

31 Physiological mechanisms also play an important role in regulating reproductive expen-  
32 ditures during periods of high-risk. Diverse mammals (47 species in 10 families) exhibit  
33 delayed implantation whereby females postpone fetal development (blastocyst implantation)  
34 to time with accumulation of nutritional reserves (Mead, 1989; Sandell, 1990). Furthermore,  
35 many mammals (including humans) suffer irregular menstrual cycling and higher abortion  
36 rates during periods of nutritional stress (Bulik et al., 1999; Trites and Donnelly, 2003). In  
37 the extreme case of unicellular organisms, nutrition is unavoidably linked to reproduction  
38 because the nutritional state of the individual regulates all aspects of the cell cycle (Glazier,

39 2009). The existence of so many independently evolved mechanisms across such a diverse  
40 suite of organisms points to the importance and universality of the fundamental tradeoff  
41 between somatic and reproductive investment, however the dynamic implications of these  
42 constraints are unknown.

43 The mechanisms by which different organisms avoid or delay reproduction during times  
44 of nutritional stress has received tremendous empirical and theoretical attention owing to  
45 the importance of these activities in shaping life-history (Cody, 1966; Martin, 1987; Man-  
46 gel and Clark, 1988). Less well understood is how resource limitation and these behav-  
47 ioral/physiological tradeoffs affect dynamics at the level of the population. Traditional  
48 Lotka-Volterra models assume a dependence of consumer population growth rates on resource  
49 density, thus *implicitly* incorporating the requirement of resource availability for reproduc-  
50 tion (Murdoch et al., 2003). Although this implicit dependence connects resource limitation  
51 to lower consumer growth rates, the following biological realities are not included: *i*) some  
52 individuals experience nutritional stress at a given time and under a given set of external  
53 conditions, while others do not; those that do have multiple pathways enabling reproductive  
54 cessation; *ii*) the portion of the population that is not nutritionally stressed is expected to  
55 reproduce at a near-constant rate and this is – averaged across species – determined strongly  
56 by body size (Kempes et al., 2012); *iii*) the rates that individuals transition from nutrition-  
57 ally poor to replete states and back have different metabolically-constrained timescales that  
58 can lead to reproductive lags. Importantly, the exclusion of these biological details may have  
59 important dynamic shortcomings, masking the effects of starvation on consumer population  
60 dynamics.

61 Resource limitation and the subsequent effects of starvation may be alternatively ac-  
62 counted for *explicitly*, such that reproduction is permitted only for individuals with sufficient

63 energetic reserves. Though straightforward conceptually, incorporating the energetic dynam-  
64 ics of individuals (Kooijman, 2000) into a population-level framework (Kooijman, 2000; Sousa  
65 et al., 2010) presents numerous mathematical obstacles (in particular a lack of smoothness,  
66 or differentiability; Diekmann and Metz, 2010), and often suffers from over-fitting due to  
67 an overabundance of parameters. These issue have limited the development of theoretical  
68 models that may aid our understanding of the effects of such tradeoffs on population dynam-  
69 ics. An alternative approach to individual-to-population frameworks is redirecting focus to  
70 macroscale relationships guiding somatic vs. reproductive investment in a consumer-resource  
71 system.

72 Here we explore how the energetic tradeoff between maintaining and building somatic  
73 tissue vs. reproduction can influence the dynamics of populations, and how such dynamics  
74 may be determined by allometric constraints. We begin by establishing a simple Nutritional  
75 State-structured population Model (NSM), where consumer starvation, and cessation of  
76 reproduction, is the consequence of resource limitation. Similarly, recovery from the starved  
77 to a reproductive state increases with resource density. Importantly, the rate at which  
78 consumers decline and recover from a starved state is wholly constrained by metabolism. By  
79 relating different rate constants to allometric constraints, we uncover important relationships  
80 between the timescales of physiological and reproductive processes, and show how organisms  
81 of different body sizes and taxonomic affinities may be prone to alternative dynamics.

82 We show that rates of starvation and recovery tend to result in systems with stable,  
83 non-cyclic fixed points and that the ratio between the rate of starvation and recovery may  
84 – in part – contribute to lower size limitations. Moreover, larger consumer body size results  
85 in rates that are less prone to cyclic dynamics than are rates for smaller organisms, pointing  
86 to potential empirical verification of the NSM framework. Finally, we show that rates of

87 starvation and recovery appear to be constrained to a parameter range where both transient  
 88 and equilibrial population dynamics result in the lowest risk of extinction for the consumer.  
 89 This surprising result suggests that the risks associated with different fluxes of consumers  
 90 in and out of a starved (non-reproductive) state may serve as an important selective driver  
 91 over evolutionary time.

92 **Starvation dynamics**

93 We integrate the somatic/reproductive tradeoff into the dynamics of a consumer-resource  
 94 system by dividing the consumer population into discrete energetic states, the occupation of  
 95 each being contingent on the consumption of a single resource  $R$ . In the NSM there are only  
 96 two energetic states for the consumer population: *i*) an energetically replete (full) state  $F$ ,  
 97 where the consumer reproduces at a constant rate  $\lambda$ , and *ii*) an energetically deficient (hun-  
 98 gry) state  $H$ , where reproduction is suppressed, and mortality occurs at rate  $\mu$ . Consumers  
 99 transition from state  $F$  to state  $H$  by starvation at rate  $\sigma$  and in proportion to the lack of  
 100 resources  $(1 - R)$ . Conversely, consumers recover from state  $H$  to the full state  $F$  at rate  $\rho$   
 101 and in proportion to  $R$ . The resource has logistic growth with a linear growth rate  $\alpha$  and  
 102 a carrying capacity of unity. Resources are eliminated by the consumer in both states: by  
 103 energetically deficient consumers at rate  $\rho$ , and by energetically replete consumers at rate  $\beta$ .

104 Accordingly, the system of equations is written

$$\dot{F} = \lambda F + \rho RH - \sigma(1 - R)F,$$

$$\dot{H} = \sigma(1 - R)F - \rho RH - \mu H,$$

$$\dot{R} = \alpha R(1 - R) - R(\rho H + \beta F).$$

105 There are three steady states for the NSM: two trivial fixed points at  $(R^* = 0, H^* =$   
106  $0, F^* = 0)$  and  $(R^* = 1, H^* = 0, F^* = 0)$ , and one non-trivial internal fixed point at

$$F^* = \frac{\alpha\lambda\mu(\mu + \rho)}{(\lambda\rho + \mu\sigma)(\lambda\rho + \mu\beta)},$$
$$H^* = \frac{\alpha\lambda^2(\mu + \rho)}{(\lambda\rho + \mu\sigma)(\lambda\rho + \mu\beta)},$$
$$R^* = \frac{\mu(\sigma - \lambda)}{\lambda\rho + \mu\sigma}.$$

107 Because there is only one internal fixed point, as long as it is stable the population trajectories  
108 will serve as a global attractor for any set of positive initial conditions. In a multidimensional  
109 system, linear stability is determined with respect to the Jacobian Matrix  $\mathbf{J}|_*$  (where  $|_*$   
110 denotes evaluation at the internal steady state), where each element of the matrix is defined  
111 by the partial derivative of each differential equation with respect to each variable. If the  
112 parameters of  $\mathbf{J}|_*$  are such that the real part of its leading eigenvalue is  $< 0$ , then the system  
113 is stable to small pulse perturbations.

#### 114 Allometric constraints

115 Our model explores a wide variety of possible dynamics yet we have not described the realistic  
116 regimes occupied by organisms where the challenge is to constrain the covariation of rates.  
117 Allometric scaling relationships highlight common constraints and average trends across large  
118 ranges in body size and species diversity. Many of these relationships can be derived from a  
119 small set of assumptions and below we describe a framework for the covariation of timescales  
120 and rates across the range of mammals for each of the key parameters of our model. We are  
121 able to define the regime of dynamics occupied by the entire class of mammals along with  
122 the key differences between the largest and smallest mammals.

123        Nearly all of the rates described in the NSM are to some extent governed by consumer  
124      metabolism, and thus can be estimated based on known allometric constraints. The scal-  
125      ing relationship between an organism's metabolic rate  $B$  and its body size at reproductive  
126      maturity  $M$  is well documented (West et al., 2002) and plays a central role in a variety of  
127      scaling relationships. Organismal metabolic rate  $B$  is known to scale as  $B = B_0 M^\eta$ , where  $\eta$   
128      is the scaling exponent, generally assumed to be 3/4 for metazoans, and varies in unicellular  
129      species between  $\eta \approx 1$  in eukaryotes and  $\eta \approx 1.76$  in bacteria (?). Several efforts have shown  
130      how a partitioning of this metabolic rate between growth and maintenance purposes can be  
131      used to derive a general equation for the growth trajectories and growth rates of organisms  
132      ranging from bacteria to metazoans (Kempes et al., 2012). More specifically, the interspecific  
133      trends in growth rate can be approximated by  $\lambda = \lambda_0 M^{\eta-1}$ . This relationship is derived  
134      from the simple balance

$$B_0 m^\eta = E_m \frac{dm}{dt} + B_m m \quad (-1)$$

135    [a and b notation — these parameters are easily measured bioenergetic parameters which  
136    are often approximately invariant across organisms of vastly different size. Our notation  
137    seeks to illustrate that the allometric model fundamentally depends on a small number of  
138    free parameters.] where  $E_m$  is the energy needed to synthesize a unit of mass,  $B_m$  is the  
139    metabolic rate to support an existing unit of mass, and  $m$  is the mass at any point in  
140    development. It is useful to explicitly write this balance because it can also be modified  
141    to understand the rates of both starvation and recovery from starvation. [Spell out the  
142    connection to nutritional state more explicitly] [As we will see it is possible to derive both  
143    sigma and rho from this balance]

144    For the rate of starvation, we make the simple assumption that an organism must meet

<sup>145</sup> its maintenance requirements using digested mass as the sole energy source. This assumption  
<sup>146</sup> implies the simple metabolic balance

$$\frac{dm}{dt} E'_m = -B_m m \quad (-1)$$

<sup>147</sup> where  $E'_m$  is the amount of energy stored in a unit of existing body mass which may differ  
<sup>148</sup> from  $E_m$ , the energy required to synthesis a unit of biomass. Give the adult mass,  $M$ , of an  
<sup>149</sup> organism this energy balance prescribes the mass trajectory of a starving organism:

$$m(t) = M e^{-B_m t / E'_m}. \quad (-1)$$

<sup>150</sup> Considering that only certain tissues can be digested for energy, for example the brain cannot  
<sup>151</sup> be degraded to fuel metabolism, we define the rate for starvation and death by the timescales  
<sup>152</sup> required to reach specific fractions of normal adult mass. We define  $m_{starve} = \epsilon M$  where it  
<sup>153</sup> could be the case that organisms have a systematic size-dependent requirement for essential  
<sup>154</sup> tissues, such as the minimal bone or brain mass. For example, considering the observation  
<sup>155</sup> that body fat in mammals scales with overall body size according to  $M_f = f_0 M^\gamma$ , and  
<sup>156</sup> assuming that once this mass is fully digested the organism begins to starve, would imply  
<sup>157</sup> that  $\epsilon = 1 - f_0 M^\gamma / M$ . Taken together the time scale for starvation is given by

$$t_\sigma = -\frac{E_m \log(\epsilon)}{B_m}. \quad (-1)$$

<sup>158</sup> The starvation rate is  $\sigma = 1/t_\sigma$ , which implies that  $\sigma$  is independent of adult mass if  $\epsilon$  is a  
<sup>159</sup> constant, and if  $\epsilon$  does scale with mass, then  $\sigma$  will have a factor of  $1/\log(1 - f_0 M^\gamma / M)$ .  
<sup>160</sup> In either case  $\sigma$  does not have a simple scaling with  $\lambda$  which is important for the dynamics

161 that we later discuss.

162 The time to death should follow a similar relationship, but defined by a lower fraction  
163 of adult mass,  $m_{death} = \epsilon' M$ . Consider, for example, that an organism dies once it has  
164 digested all fat and muscle tissues, and that muscle tissue scales with body mass according  
165 to  $M_{mm} = mm_0 M^\zeta$ , then  $\epsilon' = 1 - (f_0 M^\gamma + mm_0 M^\zeta) / M$ . Muscle mass has been shown to  
166 be roughly proportional to body mass ? in mammals and thus  $\epsilon'$  is effectively  $\epsilon$  minus a  
167 constant. Thus

$$t_\mu = -\frac{E_m \log(\epsilon')}{B_m} \quad (-1)$$

168 and  $\mu = 1/t_\mu$ .

169 It should be noted that we have thus far used mammalian allometry to describe the  
170 size-based relationships for growth, starvation, and death. However, our presentation is  
171 general, and other functional forms for  $\epsilon$ , for example, could be determined for other classes  
172 of organisms. Considering bacteria, we might expect that starvation or death is defined  
173 by the complete digestion of proteins, and in Table ?? we provide all parameter values for  
174 bacteria which we later use as a comparison in our analysis.

175 The rate of recovery  $\rho = 1/t_\rho$  requires that an organism accrues tissue from the starving  
176 state to the full state. We again use the balance given in Equation to find the timescale to  
177 return to the mature mass from a given reduced starvation mass. The general solution to  
178 Equation is given by

$$m(t) = \left[ 1 - \left( 1 - \frac{b}{a} m_0^{1-\eta} \right) e^{-b(1-\eta)t} \right]^{1/(1-\eta)} \left( \frac{a}{b} \right)^{1/(1-\eta)} \quad (-1)$$

179 with  $a = B_0/E_m$  and  $b = B_m/E_m$ . We are then interested in the timescale,  $t_\rho = t_2 - t_1$ ,  
180 which is the time it takes to go from  $m(t_1) = \epsilon M$  to  $m(t_2) = M$ , which has the final form

181 of

$$t_\rho = \frac{\log \left( 1 - \left( M \left( \frac{a}{b} \right)^{\frac{1}{\eta-1}} \right)^{1-\eta} \right) - \log \left( 1 - \left( M \epsilon \left( \frac{a}{b} \right)^{\frac{1}{\eta-1}} \right)^{1-\eta} \right)}{(\eta-1)b}. \quad (-1)$$

182 Although these rate equations are general and will hold for any organism, here we focus on  
183 parameterizations specifically for terrestrial-bound endotherms, specifically mammals, which  
184 range from  $M \approx 1$  gram (the Etruscan shrew *Suncus etruscus*) to  $M \approx 10^7$  grams (the late  
185 Eocene to early Miocene Indricotheriinae). Investigating other classes of organisms requires  
186 only substituting the energetic and scale parameters shown in Table 1, though this is beyond  
187 the current scope of our analysis, and we henceforth focus our examination on mammalian  
188 species.

### 189 **The stabilizing effects of allometric constraints**

190 Stability in the NSM is conditioned on the consumer's starvation rate  $\sigma$  relative to the its  
191 reproduction rate  $\lambda$ . As  $\sigma$  becomes less than  $\lambda$ , the resource steady state density becomes  
192 negative and extinction is inevitable. This condition  $\sigma = \lambda$  marks a transcritical (TC)  
193 bifurcation, thus marking a hard boundary below which the system becomes unphysical due  
194 to the unregulated growth of the consumer population. That the timescale of reproduction is  
195 larger than the timescale of starvation is intuitive for macroscopic organisms, as the rate at  
196 which one loses tissue due to a lack of resources is generally much faster than reproduction.  
197 In fact, allometric derivations for both reproduction (Kempes et al., 2012) and starvation  
198 (Eq. ) show that this relationship always holds for organisms within observed body size  
199 ranges. We note that the asymptote for the starvation rate at  $M \approx 8.3 \times 10^8$  defines the  
200 mass at which fat tissue accounts for 100% of organismal weight, thereby placing a hard  
201 scaling boundary on our derivation for the starvation rate.

202 In addition to the hard bound defined by the TC bifurcation, oscillating or cyclic dy-

203 namics present an implicit constraint to persistence by increasing the risk of extinction. If  
204 cycles are large, stochastic effects may result in extinction in either the consumer or resource  
205 population. In continuous-time systems, a stable limit cycle arises when a pair of complex  
206 conjugate eigenvalues crosses the imaginary axis to attain positive real parts (Guckenheimer  
207 and Holmes, 1983). This condition, known as a Hopf bifurcation, is defined by  $\text{Det}(\mathbf{S}) = 0$ ,  
208 where  $\mathbf{S}$  is the Sylvester matrix, which is composed of the coefficients of the characteristic  
209 polynomial describing the Jacobian (Gross and Feudel, 2004).

210 In addition to the onset of stable cycles, as a system with a stable fixed point nears  
211 the Hopf bifurcation, transient or decaying cycles can grow in magnitude, despite the ex-  
212 istence of a positive, non-cyclic, steady state density. Given that ecological systems exist  
213 in a state of constant perturbation (Hastings, 2001), even the onset of transient cycles that  
214 decay over time can increase the risk of extinction (Neubert and Caswell, 1997; Caswell and  
215 Neubert, 2005; Neubert and Caswell, 2009), such that the distance of a system from the  
216 Hopf bifurcation, even in the stable region, is relevant to persistence.

217 The NSM exhibits both non-cyclic as well as cyclic dynamics, and which behavior domi-  
218 nates depends strongly on the rate of starvation  $\sigma$  relative to the rate of recovery  $\rho$ . Although  
219 starvation leads to mortality risk for the individual, a moderate amount promotes persis-  
220 tence of both consumer and resource populations. Non-cyclic stability of the fixed point  
221 generally requires a higher starvation rate  $\sigma$  relative to the recovery rate  $\rho$ . The intuition  
222 behind this is that transition to the hungry (non-reproductive) state permits the resource  
223 to recover and transient dynamics to subside, whereas a low  $\sigma$  overloads the system with  
224 energetically-replete (reproducing) individuals, thus producing maintained oscillations be-  
225 tween consumer and resource (Fig. 3). However if  $\sigma$  is too large, mortality due to starvation  
226 depletes the consumer population, resulting in a lower steady state density for the consumer

227 and an opposingly higher steady state density for the resource.

228 Whereas the rate of consumer growth defines a hard bound of biological feasibility (the  
229 TC bifurcation), the rate of starvation determines the sensitivity of the consumer population  
230 to changes in resource density. While higher rates of starvation result in lower steady state  
231 population size – increasing the risk of stochastic extinction – lower rates of starvation result  
232 in a system poised near either the TC or Hopf bifurcation (or both), which will lead to  
233 elimination of the resource or the development of cyclic oscillations, respectively. Which  
234 bifurcation is approached is wholly dependent on the rate of recovery: if it is high, then  
235 cyclic dynamics will develop; if it is low, resource extinction becomes increasingly likely.

236 As the allometric derivations of NSM rate laws reveal,  $\sigma$  and  $\rho$  are not independent  
237 parameters, such that the bifurcation space shown in Fig. 3 cannot be freely navigated if as-  
238 suming biologically reasonable parameterizations. Given the parameterization for terrestrial  
239 endotherms shown in Table ?? with mass  $M$  as the only free parameter, rates of starvation  
240 and recovery are constrained to a fairly small window of potential values. We find that the  
241 allometric constraints given for terrestrial endothermic organisms confine dynamics to the  
242 steady state regime across all reasonable body size classes, which for mammals ranges from  
243 ca. 1 gram (the Etruscan shrew) to ca.  $10^7$  grams (represented by the Indricotheriinae, a  
244 subfamily of mammals living from the mid-Eocene to early Miocene). Moreover, for larger  
245 organismal mass, the distance increases between the allometric values for  $\sigma(M)$  and  $\rho(M)$   
246 relative to the Hopf bifurcation, while uncertainty in allometric parameters (20% variation  
247 around the mean; Fig. ??) results in little difference in the position of the TC and Hopf bifur-  
248 cations as well as consumer energetic rates. This result suggests 1) that small mammals are  
249 more prone to population oscillations – including both stable limit cycles as well as transient  
250 cycles – than large mammals, and 2) the decreasing distance to the Hopf bifurcation with

251 lower body sizes is suggestive of a dynamic barrier to the mass of endothermic organisms.  
252 Although the prediction of larger oscillations for animals with smaller body sizes generally  
253 holds, empirical observations of large animal population cycles are plagued by long genera-  
254 tion times and the influence of top-down effects [REFS] making direct empirical observation  
255 problematic.

256 Higher rates of starvation results in a larger flux of the population to the hungry state,  
257 eliminating reproduction and increasing the likelihood of death, however it is the rate of  
258 starvation relative to the rate of recovery that determines the long-term dynamics of the  
259 system (Fig 3). By examining the ratio  $\sigma/\rho$ , we can understand the competing effects of  
260 cyclic dynamics vs. population density on the probability of extinction. We computed the  
261 probability of extinction, which we defined as  $H(t) + F(t) = 10$  at any instant across all  
262 values of  $t > 100$  for 1000 replicates of the continuous-time system shown in Eq. XX with  
263 random initial conditions within the interval  $(R^*, H^*, F^*) \pm 100\%$  (check) for an organism  
264 of  $M = 100g$ . By allowing the rate of starvation to vary, we assessed extinction risk across  
265 a range of values for the ratio  $\sigma/\rho$  varying between  $10^{-2}$  to 2.5, thus examining a vertical  
266 cross-section of Fig. 3. As we expected, we found higher rates of extinction for both low and  
267 high values of  $\sigma/\rho$ ; for low values the higher extinction risk is the consequence of transient  
268 cycles with larger amplitudes as the system nears the Hopf bifurcation. For high values  
269 of  $\sigma/\rho$ , higher extinction risk is due to the steady decrease in the steady state consumer  
270 population density. This interplay creates an ‘extinction refuge’, such that for a relatively  
271 small range of  $\sigma/\rho$ , extinction probabilities are minimized.

272 As has been described, the  $\sigma$  vs.  $\rho$  space cannot be freely traversed, such that not all  
273 values of  $\sigma/\rho$  are biologically feasible. We observe that the allometrically constrained val-  
274 ues of  $\sigma/\rho$  (with  $\pm 20\%$  variability around the mean for the energetic parameters used to

275 determine each rate) fall within the extinction refugia, such that they are close enough to  
276 the Hopf bifurcation to avoid low steady state densities, though far enough away to avoid  
277 large-amplitude transient cycles. The fact that allometric values of  $\sigma$  and  $\rho$  fall within this  
278 relatively small window supports the possibility that a selective mechanism has constrained  
279 the physiological conditions driving observed starvation and recovery rates within popula-  
280 tions. Such a mechanism would involve a feedback between the dynamics of the population  
281 and the fitness of individuals within the population, though to what extent the dynamics of  
282 the population influence rates of starvation and recovery would also involve potential trade-  
283 offs in reproduction and somatic maintenance. Despite the possible mechanisms, our finding  
284 that allometrically-determined energetic rates place the system within this low probability  
285 of extinction region suggests that the NSM system provides general insight to a phenomena  
286 that may both drive – and constrain – natural animal populations.

287 **Minimizing extinction risk**

288

Table 1: Parameter Values For Various Classes of Organisms

	<b>Mammals</b>	<b>Unicellular Eukaryotes</b>	<b>Bacteria</b>
$\eta$	3/4		1.70
$E_m$	10695 (J gram $^{-1}$ )		10695 (J gram $^{-1}$ )
$E'_m$	$\approx E_m$		$\approx E_m$
$B_0$	0.019 (W gram $^{-\alpha}$ )		$1.96 \times 10^{17}$
$B_m$	0.025 (W gram $^{-1}$ )		0.025 (W gram $^{-1}$ )
$a$	$1.78 \times 10^{-6}$		$1.83 \times 10^{13}$
$b$	$2.29 \times 10^{-6}$		$2.29 \times 10^{-6}$
$\eta - 1$	-0.21		0.73
$\lambda_0$	$3.39 \times 10^{-7}$ (s $^{-1}$ gram $^{1-\eta}$ )		56493
$\gamma$	1.19		0.68
$f_0$	0.02		$1.30 \times 10^{-5}$
$\zeta$	1.01		
$mm_0$	0.32		

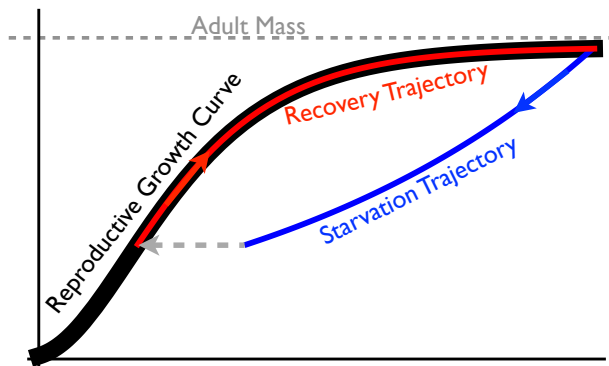


Figure 1

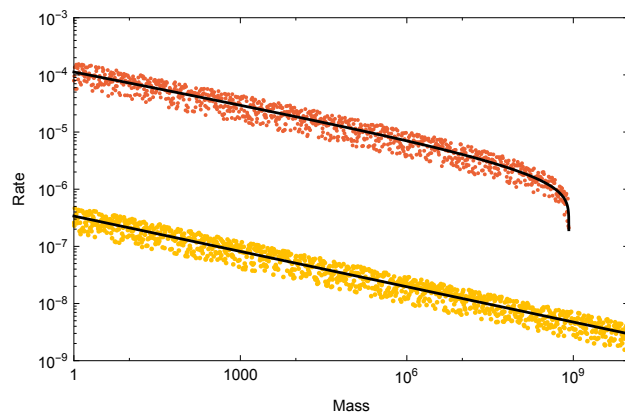


Figure 2

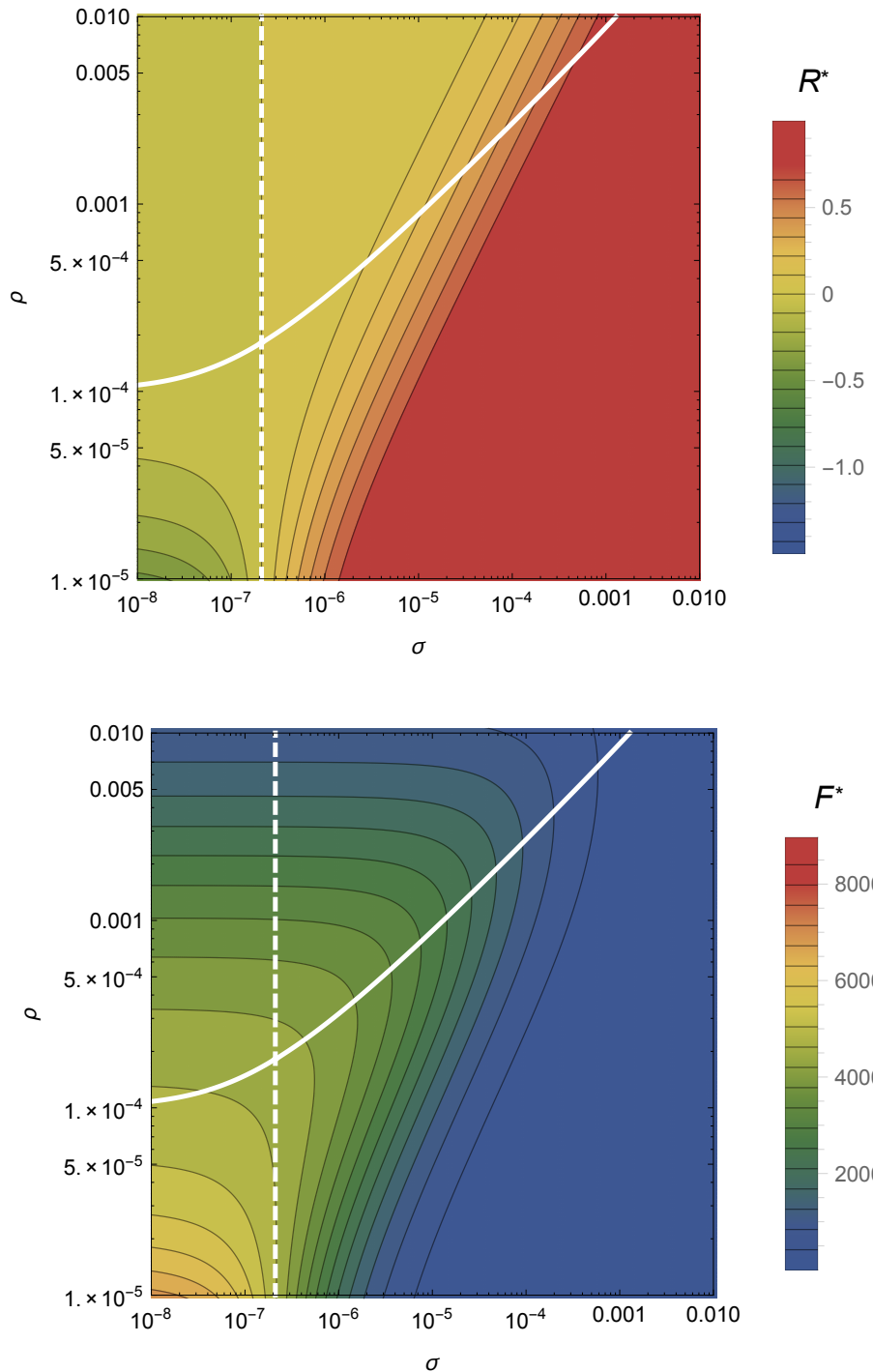


Figure 3

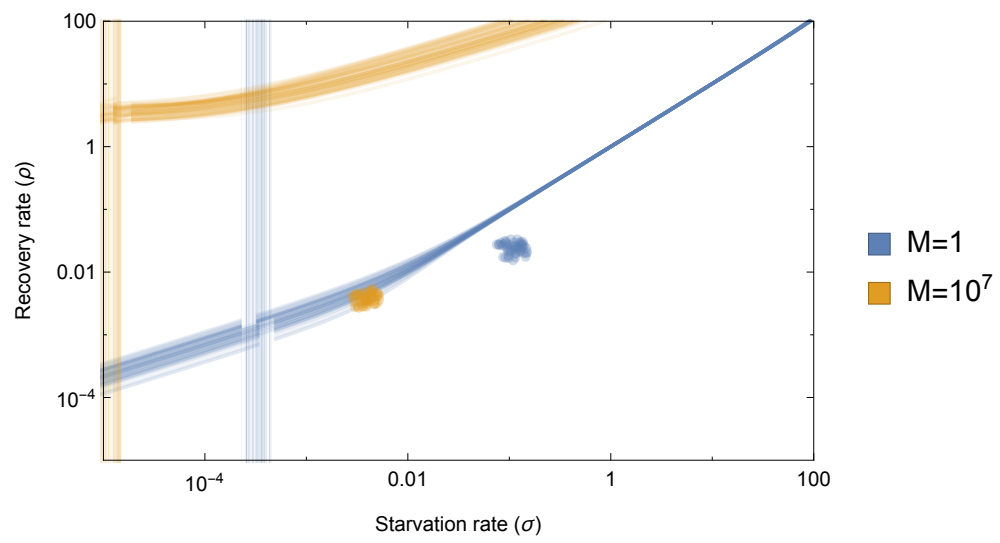


Figure 4

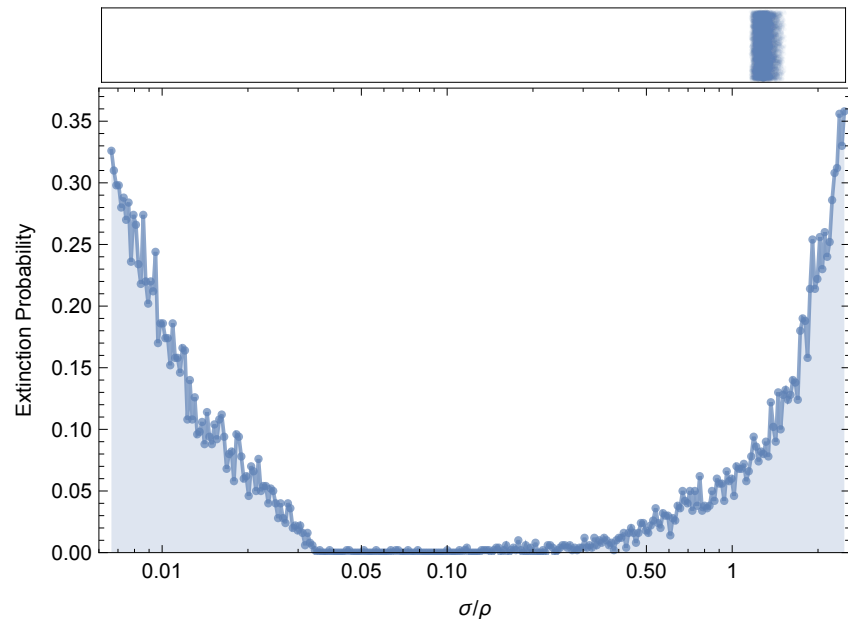


Figure 5

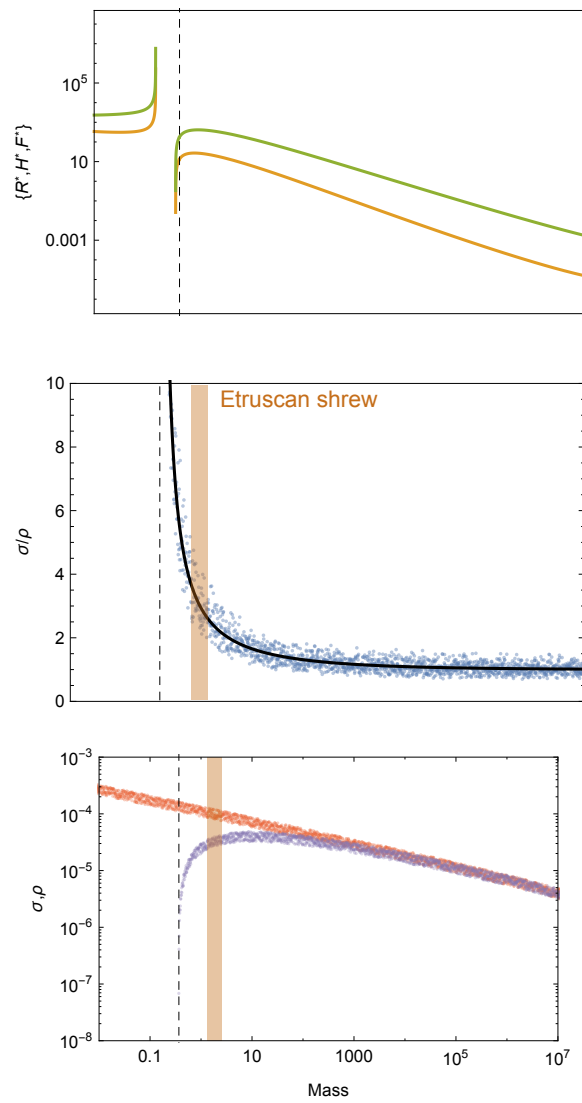


Figure 6

<sup>289</sup> **References**

- <sup>290</sup>  
<sup>291</sup> Barboza, P. and Jorde, D. (2002). Intermittent fasting during winter and spring affects body  
<sup>292</sup> composition and reproduction of a migratory duck. *J Comp Physiol B*, 172(5):419–434.
- <sup>293</sup> Bulik, C. M., Sullivan, P. F., Fear, J. L., Pickering, A., Dawn, A., and McCullin, M.  
<sup>294</sup> (1999). Fertility and Reproduction in Women With Anorexia Nervosa. *J. Clin. Psy-  
<sup>295</sup> chiatry*, 60(2):130–135.
- <sup>296</sup> Caswell, H. and Neubert, M. G. (2005). Reactivity and transient dynamics of discrete-time  
<sup>297</sup> ecological systems. *Journal of Difference Equations and Applications*, 11(4-5):295–310.
- <sup>298</sup> Cody, M. L. (1966). A General Theory of Clutch Size. *Evolution*, 20(2):174–184.
- <sup>299</sup> Daan, S., Dijkstra, C., Drent, R., and Meijer, T. (1988). Food supply and the annual timing  
<sup>300</sup> of avian reproduction. In *Proceedings of the International . . . .*
- <sup>301</sup> Diekmann, O. and Metz, J. A. J. (2010). How to lift a model for individual behaviour to  
<sup>302</sup> the population level? *Philos. T. Roy. Soc. B*, 365(1557):3523–3530.
- <sup>303</sup> Glazier, D. S. (2009). Metabolic level and size scaling of rates of respiration and growth in  
<sup>304</sup> unicellular organisms. *Funct. Ecol.*, 23(5):963–968.
- <sup>305</sup> Gross, T. and Feudel, U. (2004). Analytical search for bifurcation surfaces in parameter  
<sup>306</sup> space. *Physica D*, 195(3-4):292–302.
- <sup>307</sup> Guckenheimer, J. and Holmes, P. (1983). *Nonlinear oscillations, dynamical systems, and  
<sup>308</sup> bifurcations of vector fields*. Springer, New York.

- <sup>309</sup> Hastings, A. (2001). Transient dynamics and persistence of ecological systems. *Ecol. Lett.*,  
<sup>310</sup> 4(3):215–220.
- <sup>311</sup> Jacot, A., Valcu, M., van Oers, K., and Kempenaers, B. (2009). Experimental nest site lim-  
<sup>312</sup> itation affects reproductive strategies and parental investment in a hole-nesting passerine.  
<sup>313</sup> *Animal Behaviour*, 77(5):1075–1083.
- <sup>314</sup> Kempes, C. P., Dutkiewicz, S., and Follows, M. J. (2012). Growth, metabolic partitioning,  
<sup>315</sup> and the size of microorganisms. *PNAS*, 109(2):495–500.
- <sup>316</sup> Kirk, K. L. (1997). Life-History Responses to Variable Environments: Starvation and Re-  
<sup>317</sup> production in Planktonic Rotifers. *Ecology*, 78(2):434–441.
- <sup>318</sup> Kooijman, S. A. L. M. (2000). *Dynamic Energy and Mass Budgets in Biological Systems*.  
<sup>319</sup> Cambridge.
- <sup>320</sup> Mangel, M. and Clark, C. W. (1988). *Dynamic Modeling in Behavioral Ecology*. Princeton  
<sup>321</sup> University Press, Princeton.
- <sup>322</sup> Martin, T. E. (1987). Food as a Limit on Breeding Birds: A Life-History Perspective. *Annu.*  
<sup>323</sup> *Rev. Ecol. Syst.*, 18:453–487.
- <sup>324</sup> Mduma, S. A. R., Sinclair, A. R. E., and Hilborn, R. (1999). Food regulates the Serengeti  
<sup>325</sup> wildebeest: a 40-year record. *J. Anim. Ecol.*, 68(6):1101–1122.
- <sup>326</sup> Mead, R. A. (1989). The Physiology and Evolution of Delayed Implantation in Carnivores.  
<sup>327</sup> In *Carnivore Behavior, Ecology, and Evolution*, pages 437–464. Springer US, Boston, MA.
- <sup>328</sup> Moore, J. W., Yeakel, J. D., Peard, D., Lough, J., and Beere, M. (2014). Life-history diversity

- 329 and its importance to population stability and persistence of a migratory fish: steelhead  
330 in two large North American watersheds. *J. Anim. Ecol.*
- 331 Morgan, M. J., Wilson, C. E., and Crim, L. W. (1999). The effect of stress on reproduction  
332 in Atlantic cod. *Journal of Fish Biology*, 54(3):477–488.
- 333 Morris, D. W. (1987). Optimal Allocation of Parental Investment. *Oikos*, 49(3):332.
- 334 Murdoch, W. W., Briggs, C. J., and Nisbet, R. M. (2003). *Consumer-resource Dynamics*.  
335 Monographs in population biology. Princeton University Press.
- 336 Neubert, M. and Caswell, H. (1997). Alternatives to resilience for measuring the responses  
337 of ecological systems to perturbations. *Ecology*, 78(3):653–665.
- 338 Neubert, M. and Caswell, H. (2009). Detecting reactivity. *Ecology*.
- 339 Sandell, M. (1990). The Evolution of Seasonal Delayed Implantation. *The Quarterly Review  
340 of Biology*, 65(1):23–42.
- 341 Sousa, T., Domingos, T., Poggiale, J. C., and Kooijman, S. A. L. M. (2010). Dynamic energy  
342 budget theory restores coherence in biology. *Philos. T. Roy. Soc. B*, 365(1557):3413–3428.
- 343 Threlkeld, S. T. (1976). Starvation and the size structure of zooplankton communities.  
344 *Freshwater Biol.*, 6(6):489–496.
- 345 Trites, A. W. and Donnelly, C. P. (2003). The decline of Steller sea lions *Eumetopias jubatus*  
346 in Alaska: a review of the nutritional stress hypothesis. *Mammal Review*, 33(1):3–28.
- 347 Tveraa, T., Fauchald, P., Henaug, C., and Yoccoz, N. G. (2003). An examination of a com-  
348 pensatory relationship between food limitation and predation in semi-domestic reindeer.  
349 *Oecologia*, 137(3):370–376.

- <sup>350</sup> Weber, T. P., Ens, B. J., and Houston, A. I. (1998). Optimal avian migration: A dynamic  
<sup>351</sup> model of fuel stores and site use. *Evolutionary Ecology*, 12(4):377–401.
- <sup>352</sup> West, G. B., Woodruff, W. H., and Brown, J. H. (2002). Allometric scaling of metabolic  
<sup>353</sup> rate from molecules and mitochondria to cells and mammals. *Proc. Natl. Acad. Sci. USA*,  
<sup>354</sup> 99 Suppl 1(suppl 1):2473–2478.